

High-resolution x-ray study of thin GaN film on SiC

A. Kazimirov^{a)}

Department of Material Science and Engineering and Material Research Center,
Northwestern University, Evanston, Illinois 60208

N. Faleev and H. Temkin

Electrical Engineering Department, Texas Technical University, Lubbock, Texas 79409

M. J. Bedzyk

Department of Material Science and Engineering and Material Research Center,
Northwestern University, Evanston, Illinois 60208 and Material Science Division,
Argonne National Laboratory, Argonne, Illinois 60439

V. Dmitriev and Yu. Melnik

TDI, Inc., Gaithersburg, Maryland 20877

(Received 8 December 2000; accepted for publication 16 February 2001)

The x-ray standing wave method (XSW) and high-resolution x-ray diffraction were used to study the structural perfection and polarity of GaN epitaxial thin film grown by hydride vapor phase epitaxy on the Si-face SiC substrate. The x-ray standing wave was generated inside the 300 nm thin film under the condition of Bragg diffraction from the film. Excellent crystalline quality of the GaN film was revealed by both x-ray techniques. The XSW analysis of the angular dependencies of the Ga-K fluorescence yield measured while scanning through the GaN(0002) diffraction peak unambiguously showed the Ga polarity of the film. Correlation between the mosaic structure and the static Debye-Waller factor of the GaN lattice was also studied. © 2001 American Institute of Physics. [DOI: 10.1063/1.1364644]

I. INTRODUCTION

The structural quality of GaN epitaxial films continues to limit applications of this technologically important wide direct band-gap semiconductor.¹ A variety of substrates such as GaAs, sapphire, ZnO, SiC, Si, LiGaO, AlMgO have been used for epitaxial growth of group III nitrides. Most of these substrates have a very large lattice mismatch with GaN leading to a high density of structural defects in the film. Among these substrates SiC is characterized by a small lattice mismatch of 3.5% vs 13.8% for sapphire, the most commonly used substrate. The growth of high-quality GaN films on SiC substrates by metalorganic chemical vapor deposition (MOCVD) and molecular beam epitaxy (MBE) usually requires an AlN buffer layer.^{2,3} Recently, direct growth of high-quality GaN on SiC substrates by hydride vapor phase epitaxy (HVPE) was reported.^{4,5}

The polarity of the epitaxial film is the other fundamental issue that strongly depends on the growth technique and type of substrate. Having its origin in the noncentrosymmetric bulk crystal structure, the polarity of the GaN film determines many of the physical, chemical, and surface properties such as chemical stability,⁶ piezoelectric effect,⁷ surface morphology, and surface reconstructions.⁸

It is well known that wurtzite GaN epitaxial films are usually grown either along the [0001] or [000 $\bar{1}$] crystallographic axes. These opposing polarities differ by the se-

quence of atomic layering. By convention, in the (0001) oriented GaN film the Ga atoms occupy the top (with respect to the surface of the film) half of the atomic double layer. A (0001) film is also referred to as a Ga face, or Ga-polarity film [Fig. 1(a)]. In the lattice of the N-face GaN film the Ga atoms occupy the bottom half of the double layer [Fig. 1(b)]. Reliable determination of the polarity of GaN films grown by different techniques presents a challenging experimental problem. Experimental results obtained by different techniques are very often contradictory and inconclusive. A recent comprehensive review of different techniques used to determine polarity of GaN films can be found in Ref. 9.

The hexagonal, 6H, modification of SiC has a structure very similar to that of GaN.¹⁰ The (0001) surface is polar with either Si or C termination. The polarity of the growing GaN film depends on the polarity of the substrate and opposite for Si and C surfaces. An x-ray photoelectron spectroscopy study of GaN films grown by metalorganic vapor phase epitaxy (MOVPE) on both faces showed that GaN epitaxial films on Si and C faces of SiC are terminated by nitrogen and gallium atomic layers, respectively.¹¹ A high-resolution electron microscopy study of the AlN/SiC interface gave the opposite result, i.e., the Al-face AlN was found on the Si face of the SiC.¹² The latter result is in agreement with *ab initio* energetics calculations.¹³

It is generally accepted that a direct method to determine polarity is needed to establish the basic characteristics of polar surfaces of GaN thin films.⁹ The x-ray standing wave (XSW) method based on using the standing wave as an

^{a)}Author to whom correspondence should be addressed; electronic mail: ayk7@cornell.edu; present address: Cornell High Energy Synchrotron Source, Cornell University, Ithaca, NY 14853.

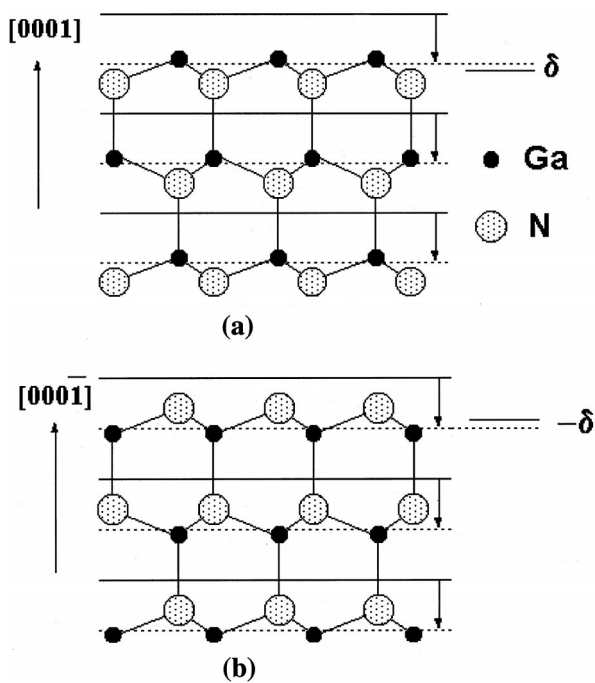


FIG. 1. Crystal structure of GaN for Ga- (a) and N- (b) faces. Ga atoms are shown as black circles, N- atoms are shown as larger circles. The positions of the antinodal XSW planes at the low angle side of the rocking curve are shown as solid lines and at the high angle side of the RC as dashed lines. The downward pointing arrows indicate the inward shift of the antinode by half of d_{0002} while crossing the GaN(0002) Bragg peak. Due to the difference in the atomic scattering factors for Ga and N atoms the diffraction planes are shifted by δ from the center of the double layer towards heavier Ga atoms (Ref. 21).

atomic scale “yardstick” to probe the atomic structure of the lattice can be regarded as one of the most “direct” techniques to determine polarity. Kazimirov *et al.*¹⁴ applied this method to study a thin GaN film grown by plasma-induced MBE on sapphire and found the polarity to be opposite to one of the MOCVD grown films. This finding has led to the study of the polarization induced properties of 2D electron gas in AlGa_n/GaN heterostructures.⁷ Recently, this technique was also used to study polarity of thin ferroelectric films.¹⁵ In this work we combined the XSW method with high-resolution x-ray diffraction to study the crystalline perfection and the polarity of the GaN epitaxial film grown by the hydride vapor phase epitaxy on Si-face SiC.

II. EXPERIMENTS

The GaN epitaxial layer was grown by HVPE.⁴ The HVPE process was performed in an inhouse built growth chamber equipped with a resistively heated furnace. In a horizontal open-flow reactor, HCl gas reacted with liquid Ga to form GaCl gas, which was transported to the growth zone of the reactor and reacted with NH₃, resulting in GaN deposition on SiC substrate. Ar was used as a carrier gas. The GaN layer was grown directly without any buffer layer⁵ on the (0001)Si face of commercial 6H-SiC on-axis 2-in.-diameter wafer. The thickness of the GaN layer was about 300 nm. The growth temperature was near 1020 °C. The GaN growth rate was about 300 nm/min.

X-ray diffraction was performed by using an X’Pert diffractometer (Philips) in triple- and double-axis geometries with Cu $K\alpha$ radiation. A four-crystal Bartels Ge(220) monochromator and a three-bounce Ge(220) analyzer crystal were used for high-resolution measurements. The analyzer crystal significantly reduced the contribution of diffuse scattering and the background, thus allowing the measurement of essentially the coherent part of the scattered x-ray intensity. The x-ray diffraction curves measured with wide-opened detector and without analyzer crystal will be referred to here as x-ray rocking curves (RC).

The XSW measurements were performed at the beam-line X15A of the National Synchrotron Light Source. The energy of the incident beam was tuned to 11.0 keV by a double crystal Si(111) monochromator. The incident beam slit was narrowed to 1 mm horizontally and 0.05 mm vertically. The sample was mounted on a two-circle diffractometer. An energy dispersive solid-state detector was used to collect x-ray fluorescence spectra from the sample. Simultaneously, the intensity of the diffracted x-ray beam was measured with NaI scintillation detector. The Ga-K fluorescence yield from the film was measured as a function of the incident angle while scanning through the GaN(0002) Bragg reflection. The XSW data were collected from five different spots on the sample characterized by different degrees of mosaic spread.

III. RESULTS AND DISCUSSION

The x-ray diffraction measurements revealed very high crystalline quality of the film. The coherent GaN(0002) and (0004) ω - 2θ x-ray diffraction curves (where the ω angle refers to the sample and the θ angle to the analyzer) measured with a Ge(220) three-bounce analyzer crystal show the characteristic interference pattern (Fig. 2). The interference fringes are more pronounced for the (0002) reflections but are clearly observed also in the vicinity of the (0004) Bragg peak. Determination of the thickness of the film from the width of the (0002) peak and from the period of the oscillations gave the value of 300 nm in good agreement with what was expected from the growth rate. From the angular width of the interference pattern for the (0002) reflection the thickness variations due to the roughness of the film can be estimated as 30 nm. The c -lattice constant was determined to be 5.177 Å. This is lower than the value of 5.1854 Å reported in Ref. 16 for GaN grown on SiC.

The coherent (0002) ω curve measured by scanning the sample through the diffraction peak while keeping the analyzer crystal fixed at the position of the maximum intensity has a shape typical for a layer containing large mosaic blocks [see Fig. 2(a)]. Our analysis gives an average size of the blocks as 1 μ m. This mosaic spread is the main reason for the broadening of the double-crystal rocking curves. The estimations of the density of dislocations from the ω curves give the value of 2 – 4×10^7 cm⁻² for the threading dislocations density and one order of magnitude more for the density of edge dislocations with the Burgers vectors in the (0001) plane. These are unusually low values considering the lattice mismatch and the thickness of the film. These results

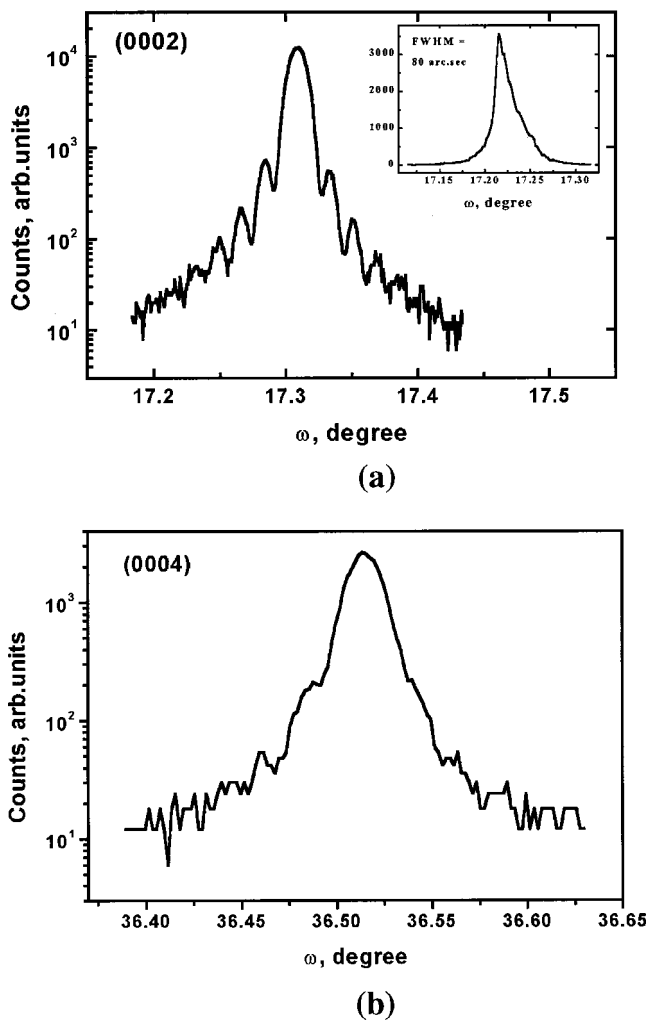


FIG. 2. Experimental (0002) and (0004) x-ray ω - 2θ diffraction curves measured from the 300 nm thick GaN film on SiC substrate by using the high-resolution x-ray diffractometer in triple-axis geometry. A Ge(220) three-bounce analyzer crystal was used to measure primarily the coherent component of the scattered x-ray intensity by significantly reducing the contribution of the diffuse scattered intensity. Inset (a) shows the coherent (0002) ω curve measured at a fixed 2θ for the analyzer crystal. The interference fringes are clearly seen in both (0002) and (0004) curves indicating the excellent crystalline quality of the film.

are in good agreement with our TEM analysis showing low dislocation density and large areas nearly free of defects.

The interesting feature derived from diffraction measurements is that the coherent lengths for the (0002) and the (0004) reflections are very close to each other (295 and 255 nm) and to the thickness of the film. This is characteristic for the epitaxial layers with low defect density and indicates the absence of elastic strain due to deviations of the lattice constant from its average value.

A typical experimental XSW data set is shown in Fig. 3(a). The characteristic minimum and maximum of the Ga K fluorescence yield are observed at the low and high angle side of the rocking curve due to the movement of the XSW pattern while scanning the sample through the GaN (0002) diffraction peak.

Neglecting the extinction effect the fluorescence yield from the j th sublattice of the compound crystal can be written as¹⁷

$$Y_H^j(\theta) = 1 + R(\theta) + 2\sqrt{R(\theta)}|S_H^j|e^{-M_H^j - W_H^j} \times \cos[\nu(\theta) - \varphi_H^j],$$

where $|S_H^j|$ and φ_H^j are the modulus and the phase of the geometrical structural factor of the j th sublattice $S_H^j = |S_H^j|e^{i\varphi_H^j} = \sum_n \exp(i\mathbf{H}\mathbf{r}_n^j)$, $e^{-M_H^j}$ and $e^{-W_H^j}$ are the thermal and static Debye-Waller factors; and $\nu(\theta)$ is the phase of the complex E -field amplitude ratio E_H/E_0 . Thus both the modulus and the phase of the structure factor of the individual sublattice can be measured in the XSW experiment making the method phase sensitive. Since the phase of the Ga sublattice is different for the Ga- and N-polar GaN crystals the polarity can be directly determined by analyzing the Ga-K fluorescence yield curve.

For over two decades the XSW technique was applied to the study of surface structures of nearly perfect crystals.¹⁸ Recently, this method has been extended to compound thin films with the thicknesses less than the extinction length, i.e., when the x-ray diffraction becomes kinematical.^{14,15,19,20} The standing wave in thin film is generated via the interference between the strong incident wave and the weak kinematically diffracted wave from the film resulting in much weaker XSW modulations in comparison with perfect bulk crystals. One distinct advantage of the thin film XSW method is the broadening of the rocking curve that makes it possible to study a variety of crystalline materials that cannot be grown as bulk perfect crystals. The absence of the extinction effect makes it possible to account for the broadening of the rocking curve due to mosaic structure by performing a convolution with a Gaussian function.¹⁹

The imperfection of the crystal lattice generating the x-ray standing wave is characterized by a static Debye-Waller (DW) factor $e^{-W_H^j}$. This factor tells us which fraction of the crystal lattice is scattering coherently; the remainder $(1 - e^{-W_H^j})$ of the lattice is contributing to the diffuse scattered intensity. This assumes that the crystal lattice is still perfect but its scattering power is reduced by the factor of $e^{-W_H^j}$. The static DW factor equals unity for a perfect crystal and zero for an amorphous material. The x-ray standing wave is generated by the coherent part of the crystal lattice.

The basic features of the (0002) XSW behavior in a wurtzite GaN lattice are shown in Fig. 1. The x-ray standing wave is generated inside the film via the interference between the incident and the (0002) Bragg diffracted x-ray beams. It has the periodicity of the GaN diffraction planes (d_{0002}) and the planes of the maximum and minimum of the electric field intensity are parallel to the atomic planes. Scanning the crystal through the Bragg peak causes a change of the phase of the diffracted beam by π radians and, consequently, an inward shift of the standing wave by $(1/2)d_{0002}$. At the low-angle side of the diffraction peak the planes of maximum intensity, i.e., the antinodes, are located between the double atomic layers (solid lines in Fig. 1) while after crossing the Bragg peak they are positioned inside the double layer (dashed lines) at the diffraction planes. Therefore, the XSW antinodes pass through the Ga-atomic layer for Ga-polar film [Fig. 1(a)], but not for the N-polar film [Fig. 1(b)].

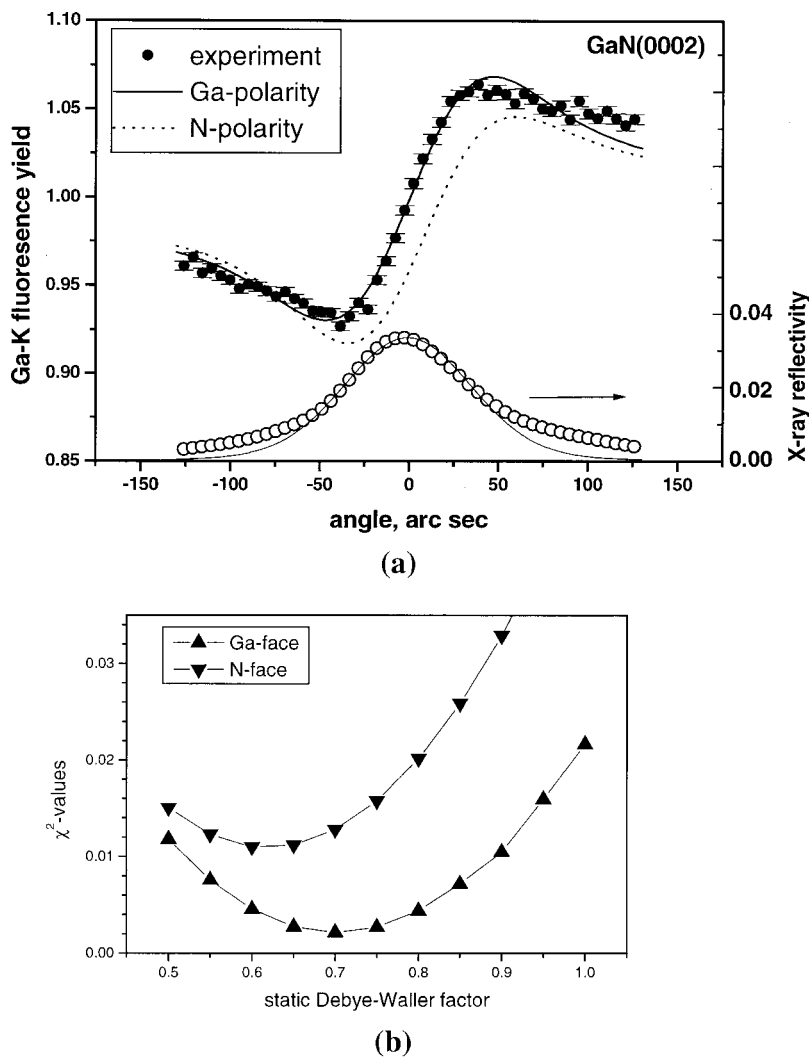


FIG. 3. (a) One of the experimental XSW data sets measured from the 300-nm-thick GaN film. The experimental x-ray reflectivity curve (bottom) is shown as open circles, the solid line is the convolution of the theoretical x-ray rocking curve with a Gaussian function with $\sigma=31.5$ arcsec. The experimental Ga-K fluorescence yield is shown at the top as solid circles; the solid line is the best fit for the Ga-face film yielding a static Debye-Waller factor $e^{-W}=0.71$. The theoretical curve for the N face is shown as a dotted line for comparison; (b) the χ^2 values as a function of the DW factor used as the only fitting parameter for the Ga face (up triangles) and N-face GaN film (down triangles). The Ga-face model gives five times lower χ^2 values than the N-face model.

Due to the difference in the atomic scattering factors for Ga and N atoms the diffraction planes inside the double layer are positioned more closely to the Ga atomic layer (for the details of the calculation of the exact location of the diffraction plane see Ref. 21). Thus, by monitoring the Ga-fluorescence angular response the polarity of the film can be identified.¹⁴

To fit the experimental XSW data the approach developed in Refs. 14 and 19 was explored. First, the theoretical x-ray reflectivity curve was convoluted with the Gaussian function to take into account the mosaic spread. For the data shown in Fig. 3(a) the $\sigma=31.5$ arcsec gives the best fit to the experimental rocking curve with the full width at half maximum (FWHM) equal to the experimental value. The same Gaussian function was then used for the convolution of the calculated fluorescence yield. Then, the Ga-K XSW fluorescence yields calculated for Ga- and N-polar GaN films were fitted to the experimental data with the static DW factor as the only fitting parameter. For the XSW calculations we used computer algorithm developed in Ref. 22 for multilayer crystalline systems. Thus, two quantities were derived from the XSW data: the polarity of the film and the static DW factor of the GaN lattice generated the standing wave.

Typical χ^2 plots for the Ga and N polarity of the film are

shown in Fig. 3(b). For all experimental data taken from different parts of the sample the XSW analysis gives significantly, from 4 to 6 times, lower χ^2 values for the Ga-face film. The best fit for the Ga-face film is shown in Fig. 3(a) by the solid line. The theoretical curve for the N-face film is also shown for comparison. Thus, our analysis unambiguously shows that the Ga-face GaN film grows on Si-face SiC substrate. This result is in agreement with the high-resolution electron microscopy data¹² and the *ab initio* energetic calculation¹³ and support the “standard framework” proposed in Ref. 9.

The broadening of the x-ray rocking curves collected during the XSW measurements is mainly due to the mosaic spread. The values of the FWHM of the x-ray RCs taken from different regions of the sample varied from 62 to 95 arcsec while dynamical diffraction theory gives the FWHM of 39 arcsec. The corresponding σ values of the Gaussian function varied from 20 to 36 arcsec. The fact that the x-ray standing wave is generated by the “coherent” part of the lattice gives us the unique opportunity to look at the correlation between the mosaic spread and the perfection of the lattice. The static DW factor derived from the XSW data as a function of the mosaic spread is presented in Fig. 4. An interesting conclusion immediately follows: the increased

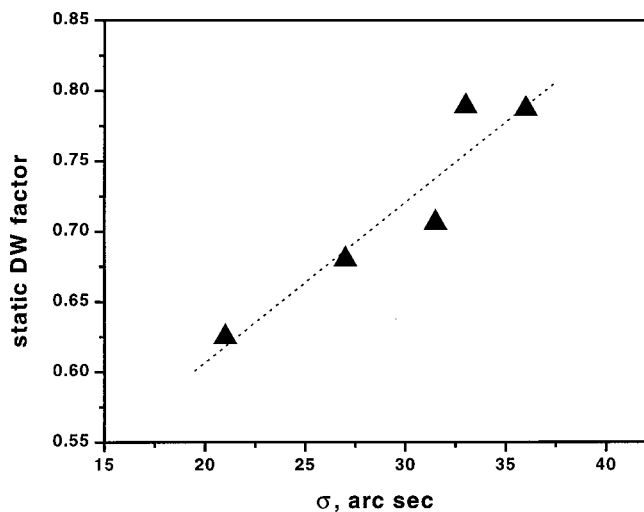


FIG. 4. Correlation between the static Debye–Waller factor of the crystal lattice determined by the x-ray standing wave technique and the broadening of the x-ray diffraction curve due to mosaic spread.

mosaic spread leads to a more perfect lattice inside individual mosaic blocks. This conclusion appears counterintuitive since the epitaxial film with broader RC should have lower structural quality. We explain this phenomenon by the getter effect of the dislocation structure on point defects generated during epitaxial growth. It is well known that dislocations work as sinks for point defects. The higher degree of mosaic spread requires higher density of dislocations in the boundaries between individual blocks. A denser dislocation structure is more effective in getting point defects from the lattice of the adjacent blocks thus leading to the higher values of the static DW factor.

This effect is very difficult to observe by standard x-ray diffraction techniques. Usually the x-ray intensity diffracted from the film can be considered as consisting of two components, different in their physical origin. The first originates from the “coherent” part of the lattice that can be described as a perfect crystal with the scattering power reduced by the static DW factor. The second part is the diffuse scattering from defects. The mosaic structure washes out the sharp coherent component of the scattered intensity resulting in the broadening of the x-ray diffraction peak. Thus, the increase in the reflectivity due to the lower density of point defects is accompanied by the broadening of the RC due to higher mosaic spread. The x-ray standing wave is the result of the interference between the incident and coherently scattered from the film waves. By measuring the fluorescence yield from atoms of the film generated by the standing wave, we can directly probe the structure of the coherent part of the atomic lattice. Here we assume that the contribution of the diffuse scattered x rays to the fluorescence yield is negligible. This assumption is based on the fact that the diffuse scattering is distributed over wide angular range while the XSW signal is measured in a narrow angular region within the width of the diffraction peak.

The results of the XSW analysis demonstrate excellent crystalline quality of the film grown by the HVPE. Indeed, the values of the static DW factor of $e^{-W} \approx 0.8$ are close to

typical values usually observed in the epitaxial semiconductor films grown by the MBE or MOCVD on GaAs.¹⁷ (For comparison, the static DW factor determined by the XSW technique for the GaN film grown by the plasma induced MBE on sapphire was $e^{-W} \approx 0.36$.¹⁴) This high degree of lattice perfection and low defect density in the film are unusual for the given lattice mismatch and the thickness of the film. The high degree of perfection can be attributed to the extremely high growth rate of about 300 nm/min. We speculate that at this rate, most parts of point defects generated near the surface during epitaxial growth do not have sufficient time to reach the interface and form misfit dislocations. Additional experiments are required to strengthen this hypothesis.

III. CONCLUSIONS

We applied high-resolution x-ray diffraction and x-ray standing wave techniques to study the structure and polarity of a GaN film grown by hydride vapor phase epitaxy on the (0001)Si face of commercial 6H–SiC crystal. In our high-resolution x-ray diffraction measurements the three-bounce Ge(220) analyzer crystal was used to reduce the contribution of diffuse scattering. The diffraction data show high crystalline quality of the film and low dislocation density. This conclusion was confirmed by TEM. We also found that the mosaic structure of the film is the main contributor to the broadening of the x-ray rocking curves.

The XSW technique explored here is based on generation of x-ray standing wave inside a thin GaN film, under condition of the (0002) diffraction from the film. The analysis of the Ga–K fluorescence yield modulations unambiguously revealed the Ga polarity of the film. This result is consistent with the high-resolution electron microscopy data¹² and the *ab initio* energetic calculations¹³ and supports the “standard framework” proposed in Ref. 9. The correlation between the perfection of the crystalline lattice measured by the static Debye–Waller factor and the degree of the mosaicity was studied by analyzing the XSW data taken from different spots on the sample. We found that the regions of the film with higher mosaic spread exhibit higher crystalline perfection. We conclude that this is due to the getter effect of dislocations on point defects generated during epitaxial growth.

The unusually low defect density in the GaN film grown by the HVPE found in this work requires further investigations. One plausible model brings into consideration very high growth rate characteristic for this technique that can possibly prevent point defects generated at the surface of the film from reaching the interface and forming misfit dislocations.

ACKNOWLEDGMENTS

This work was supported by the U. S. Department of Energy under Contract Nos. W-31-109-ENG-38 to ANL and DE-AC02-98CH10886 to NSLS and by the NSF under Contract No. DMR9973436. Research at TDI was supported by Ballistic Missiles Defense/Innovative Science and Technology and the Office of Naval Research (contract manager

Colin Wood). Work at TTU was supported by the J. F. Maddox Foundation. The authors would like to thank S. N. G. Chu of Bell Laboratory for TEM studies.

- ¹S. Nakamura and G. Fasol, *The Blue Laser Diode-GaN Based Light Emitters and Lasers* (Springer, Heidelberg, 1997).
- ²I. P. Nikitina and V. A. Dmitriev, *Inst. Phys. Conf. Ser.* **141**, 431 (1994).
- ³M. E. Lin, B. Swerdlov, G. L. Zhou, and H. Morkoc, *Appl. Phys. Lett.* **62**, 3479 (1993).
- ⁴Yu. V. Melnik, I. P. Nikitina, A. S. Zubrilov, A. A. Sitnikova, and V. A. Dmitriev, *Inst. Phys. Conf. Ser.* **142**, 863 (1996).
- ⁵Yu. V. Melnik, I. P. Nikitina, A. E. Nikolaev, and V. A. Dmitriev, *Diamond Relat. Mater.* **6**, 1532 (1997).
- ⁶C. J. Sun, P. Kung, A. Saxler, H. Ohsato, E. Bigan, M. Razeghi, and D. K. Gaskill, *J. Appl. Phys.* **76**, 236 (1994).
- ⁷O. Ambacher, J. Smart, J. R. Shealy, N. G. Weimann, K. Chu, M. Murphy, W. J. Schaff, L. F. Eastman, R. Dimitrov, L. Wittmer, M. Sturzmann, W. Rieger, and J. Hilsenbeck, *J. Appl. Phys.* **85**, 3222 (1999).
- ⁸A. R. Smith, R. M. Feenstra, D. W. Greve, J. Neugebauer, and J. E. Northrup, *Phys. Rev. Lett.* **79**, 3934 (1997).
- ⁹E. S. Hellman, *MRS Internet J. Nitride Semicond. Res.* **3**, 1 (1998).
- ¹⁰P. Käckell, B. Wenzien, and F. Bechstedt, *Phys. Rev. B* **50**, 17037 (1994).
- ¹¹T. Sasaki and T. Matsuoka, *J. Appl. Phys.* **64**, 4531 (1988).
- ¹²F. A. Ponce, C. G. Van de Walle, and J. E. Northrup, *Phys. Rev. B* **53**, 7473 (1996).
- ¹³R. Di Felice, J. E. Northrup, and J. Neugebauer, *Phys. Rev. B* **54**, R17351 (1996).
- ¹⁴A. Kazimirov, G. Scherb, J. Zegenhagen, T.-L. Lee, M. J. Bedzyk, M. K. Kelly, H. Angerer, and O. Ambacher, *J. Appl. Phys.* **84**, 1703 (1998).
- ¹⁵M. J. Bedzyk, A. Kazimirov, D. L. Marasco, T.-L. Lee, C. M. Foster, G.-R. Bai, P. L. Lyman, and D. Keane, *Phys. Rev. B* **61**, R7873 (2000).
- ¹⁶M. Leszczynski, H. Teisseyre, T. Suski, I. Grzegory, M. Bockowski, J. Jun, S. Porowski, K. Pakula, J. M. Baranowski, C. T. Foxon, and T. S. Cheng, *Appl. Phys. Lett.* **69**, 73 (1996).
- ¹⁷A. Kazimirov, M. Kovalchuk, and V. Kohn, *Sov. Tech. Phys. Lett.* **14**, 587 (1988).
- ¹⁸J. Zegenhagen, *Surf. Sci. Rep.* **18**, 199 (1993).
- ¹⁹A. Kazimirov, T. Haage, L. Ortega, A. Stierle, F. Comin, and J. Zegenhagen, *Solid State Commun.* **104**, 347 (1997).
- ²⁰A. Kazimirov, L. X. Cao, G. Scherb, L. Cheng, M. J. Bedzyk, and J. Zegenhagen, *Solid State Commun.* **114**, 271 (2000).
- ²¹M. J. Bedzyk and G. Materlik, *Phys. Rev. B* **32**, 6456 (1985).
- ²²V. Kovalchuk, V. G. Kohn, and E. F. Lobanovich, *Sov. Phys. Solid State* **27**, 2034 (1985).